Construction and Building Materials 106 (2016) 209–217

Contents lists available at ScienceDirect

Construction and Building Materials

journal homepage: www.elsevier.com/locate/conbuildmat

Effectiveness of tetra-ethyl-ortho-silicate (TEOS) consolidation of fired-clay bricks manufactured with different calcination temperatures

Patricia Martinez [a,b], Melissa Soto [a], Franco Zunino [a], Claudia Stuckrath [a], Mauricio Lopez [a,b,c,*]

[a] Department of Construction Engineering and Management, School of Engineering, Pontificia Universidad Católica de Chile, Vicuña Mackenna 4860, Casilla 30, Correo 22, Santiago, Chile
[b] Cultural Heritage Center, Pontificia Universidad Católica de Chile, Chile
[c] Sustainable Urban Development Center (CEDEUS), Pontificia Universidad Católica de Chile, Chile

HIGHLIGHTS

- All specimens treated with TEOS showed improvements in both mechanical and transport properties.
- The improvements strongly depend on porosity of the bricks, which strongly influences the retention of TEOS.
- Consolidation effectiveness also depends on the substrate–consolidant interaction (mineralogy).

ARTICLE INFO

Article history:
Received 25 May 2014
Received in revised form 18 November 2015
Accepted 16 December 2015
Available online 23 December 2015

Keywords:
Polymerization
Strength
Hardness
Porosity
Heritage
Immersion
Tetraethylorthosilicate
TEOS

ABSTRACT

Tetra-ethyl-ortho-silicate (TEOS) consolidation is a promising technique; however, the effects of substrate microstructure and mineralogy on the TEOS performance have not been systematically assessed; which is critical to improve consolidation efficiency. Clay bricks were manufactured in a variety of clay/kaolin proportions, calcination temperatures and treated with TEOS. by immersion. TEOS retentions between 4.9% and 5.9% were obtained, which increased surface hardness, compressive strength and flexural strength compared to non-treated specimens. Furthermore, consolidation reduced brick permeability and resulted in slight color variations. These improvements are explained by the deposition of consolidant in the pores and substrate–consolidant chemical interaction.

1. Introduction

Brick is one of the most ancient construction materials, and even today bricks are often used in the construction of buildings due to the low costs of their raw materials and manufacturing process [1–3]. Brick is particularly relevant because is the primary construction material used in historical buildings [4], especially in Latin America (e.g., Chile) [5] where the ceramic industry is still important [6].

One disadvantage of bricks is that they are susceptible to degradation compared to other construction materials. Bricks have a relatively high open porosity that varies between 11–40% in contemporary buildings and 30–38% in historical buildings [7]. Moreover, this porosity is interconnected, thus facilitating the transport of water and destructive agents through the brick matrix [8]. This porosity, combined with the low mechanical strength of brick (compressive strength < 20 MPa and flexural strength < 5 MPa), makes it more susceptible to degradation.

Consolidation with TEOS is widely used to restore natural stones, and it is a promising solution for the restoration of fired-clay bricks [9]. In the presence of water, ethyl silicate transforms to silanol (Si–OH) and ethanol (hydrolysis) and a polymerization reaction occurs, which generates silica gel (Si–O–Si) that precipitates inside the material, filling its microstructures (through dehydration/condensation). Silica gel also reacts with hydroxyl groups present in a material to restore its natural binding [10].

Hydrolysis is strongly influenced by relative humidity. Under conditions of high relative humidity, hydrolysis occurs quickly, leaving behind residual Si–OH that causes cracks. Under conditions

* Corresponding author at: Department of Construction Engineering and Management, School of Engineering, Pontificia Universidad Católica de Chile, Vicuña Mackenna 4860, Casilla 30, Correo 22, Santiago, Chile.
E-mail address: mlopez@ing.puc.cl (M. Lopez).

http://dx.doi.org/10.1016/j.conbuildmat.2015.12.116
0950-0618/

Nomenclature

Hem	hematite
plg (alb)	plagioclase albite
plg (ant)	plagioclase anorthite
Ill	illite
Mll	mullite
Mcv	muscovite
Qtz	quartz muscovite, illite and smectite (montmorillonite)

of low relative humidity, the hydrolyzed material does not cracks and is glassy, but high monomer evaporation occurs, reducing the final amount of polymer that precipitates in the substrate [10].

It has not been possible to identify quantitative relationships between dosages of TEOS and improvements in mechanical and transport properties, based on the microstructure characteristics of a consolidated substrate. This prevents the effective and efficient use of TEOS, not only due to cost considerations but also the lack of information regarding the expected performance of a material after treatment.

This study quantifies and evaluates the effect of TEOS on a variety of clay brick microstructures using several techniques. It identifies factors in the substrate microstructure that explain and maximize the consolidant effect, allowing the future design of consolidation treatment with TEOS.

2. Materials and methods

2.1. Preparation of clay brick specimens

Clay brick specimens with different microstructures were produced. The brick specimens were prepared with common clay from Quilicura, Santiago and kaolin from Tiltil, Chacabuco. Different proportions of clay/kaolin were used, and the calcination temperature during production was systematically changed to obtain different chemical and physical microstructures. The chemical compositions of raw materials were determined by energy dispersive spectroscopy (EDS) using an EDX-720 analyzer, and are presented in Table 1.

Clay mixtures with three different kaolin percentages by weight were used to modify the initial plasticity of the tested bricks [11] and obtain different chemical and physical microstructures: (a) 0% kaolin/100% clay (b) 10% kaolin/90% clay and (c) 20% kaolin/80% clay. Clay mixtures were places in molds and allowed to air dry for three days prior to the calcination process, which was performed at 900 °C. The temperature of 900 °C was chosen because it is a common temperature used in the manufacture of industrial bricks [2,11] and artisanal bricks for historical buildings [12,13]. A 7.5 °C/min heating rate was selected, and the bricks were kept at the maximum temperature for 4 h.

Clay bricks composed of 10% kaolin were calcined at either 800 °C, 900 °C or 1000 °C to obtain different sintering and degrees of matrix crystallization, thus achieving different porosities, pore interconnectivities and initial properties in the specimens tested [13,14]. The same firing regime was used for all bricks. A 10% kaolin content was chosen because it is a typical composition used in the manufacture of industrial bricks in Santiago [11].

Table 1
Chemical composition of raw materials determined by EDS (% by wt.).

	Clay	Kaolin
Si	56.99	53.85
Al	21.39	33.50
Fe	8.65	6.67
Ca	4.90	0.00
Mg	3.68	0.00
K	2.82	3.51
Ti	0.82	0.67
Mn	0.22	0.00
Ba	0.18	0.63
P	0.12	0.00
Sr	0.08	0.04
S	0.08	1.07
Zr	0.03	0.00
Zn	0.02	0.01
Rb	0.01	0.01
Cu	0.00	0.05

Initial water dosage was determined as the amount required to obtain the same plasticity from all clay-kaolin mixtures used. Each $4 \times 4 \times 16$ cm prismatic mold was filled by six layering steps with the aid of a metal tamper for compaction. Twelve prismatic specimens were manufactured from each mix at each calcination temperature. After calcination, specimens were placed in an environmental test chamber (RH = 50% and T = 20 °C) for one week, with the aim of reaching equilibrium with environmental humidity before applying the consolidant.

A summary of the manufacturing conditions and nomenclature used to identify the specimens is presented in Table 2.

2.2. Consolidant application

Silres OH-100 consolidant was used, which is a hydrolyzed ethyl silicate. The product's technical data sheet indicates a final 30% deposition of silica gel after 28 days and a density of 0.997 g/cm^3 at 25 °C. The consolidant was applied by immersion at room temperature for 1 h. After the immersion, specimens were drained for 30 min and placed in an environmental chamber for four weeks to allow the consolidant to cure.

2.3. Experimental procedures

2.3.1. Raw materials characterization

The mineralogies of raw materials and clay brick specimens were determined through X-Ray Diffraction (XRD) using a D2 PHASER Diffractometer from Bruker, with Cu Kα radiation in continuous scan mode, 40 kV, 20 mA, and an explored range 2θ between 0° and 50°, as this range has been found to contain the typical mineralogical forms found in clay minerals [15].

2.3.2. Consolidation effectiveness assessment

The consolidation effectiveness was assessed through the variation of mechanical and transport properties. Mechanical properties were characterized based on surface hardness, compressive strength and flexural strength.

2.3.2.1. Mechanical properties. The surface hardness was determined as the depth of penetration by a Universal Brinell durometer, Karl Frank 500 series, using a 6.4 mm (1/4") steel ball, a preload of 10 kg, and an additional load of 62.5 kg. This method was selected because it overcoming issues associated with measuring indentation on irregular surfaces such as fired-bricks. The effect of consolidation on surface hardness was assessed by considering the difference between the penetration of the ball with a load of 72.5 kg and 10 kg. Three measurements were performed on the lateral surfaces of three specimens (nine measurements in total) before and after consolidation. Lower measured values represent decreased penetration of the samples and, therefore, higher surface hardness.

Compressive strength and flexural strength tests were performed according to the UNE-EN 1926:2007 [16] and UNE-EN 12372:2007 [17] standards, respectively. Compressive strength tests were conducted on 5 cm cubic samples with the filling face of each sample oriented perpendicular to the loading axis to avoid the effects of sedimentation and preferential orientation due to the brick manufacturing process. Five samples of each mixture were tested. Flexural tests were conducted on $4 \times 4 \times 16$ cm prismatic samples following the same orientation criteria of the compressive strength tests. Three samples of each mixture were tested.

2.3.2.2. Physical and transport properties. Transport properties were characterized in six specimens by evaluating the following: open porosity (OP) according to UNE-EN-1936:2007 [18] and capillary absorption coefficient (CA) according to UNE-EN-1925:1999 [19] and ASTM C1585 [20]. Pore interconnectivity was determined

Table 2
Clay-brick manufacturing conditions and nomenclature.

		Amount of kaolin in dry mix (% by wt.)		
		0	10	20
Temperature of calcination (°C)	800	–	L10-800	–
	900	L0-900	L10-900	L20-900
	1000	–	L10-1000	–

by measuring the electrical resistivity (R) of saturated specimens at atmospheric pressure for 72 h. A Miller 400 an Analog Megohmmeter was used, applying a voltage of 12 V.

Quantitative analysis of pore size distribution was performed using a water desorption test. This test is based on the capillary phase change of water within the pores of a substrate as determined by the pore diameter [21]. The relationship between the equilibrated relative humidity and the radius of the smallest empty pore is given by the Kelvin–Laplace equation [22].

Pore sizes within the 1-to-0.01-μm range were analyzed, as these correspond to the primary active range of the SE [2]. The desorption curve was determined according to ASTM E104-02 [23] using different salt solutions for fixing certain relative humidities, as shown in Table 2.

Cubic specimens 1 cm in size, previously saturated in water for 48 h at 720 mm-Hg under vacuum, were placed in an airtight container containing a solution oversaturated with the respective salt. Saturation was conducted under vacuum to ensure the saturation of small pores in the specimens. The ambient temperature was controlled using an environmental chamber. Five specimens of each mixture were placed in the containers, and water loss was registered after 48 h using a 0.001 g precision scale. Water loss represented the volume of the pores within the specific size range given by the relative humidity.

2.3.2.3. Aesthetic properties. Color variations were determined from the chromatic coordinates (a,b) and the luminance factor (L) of the CIELAB system. A MiniScan XE Plus colorimeter was used, in the measurement range from 350 to 750 nm with a wavelength precision of ±0.5 nm. The color difference was quantified as (ΔE) as shown below:

$$\Delta E = \sqrt{(L_1^* - L_2^*)^2 + (a_1^* - a_2^*)^2 + (b_1^* - b_2^*)^2} \quad (1)$$

L_1^* = luminosity of the non-treated specimen,
a_1^* = chromatic coordinate (red-green variation) of the non-treated specimen,
b_1^* = chromatic coordinate (yellow-blue variation) of the non-treated specimen,
L_2^* = luminosity of the treated specimen,
a_2^* = chromatic coordinate (red-green variation) of the treated specimen,
b_2^* = chromatic coordinate (yellow-blue variation) of the treated specimen.

2.3.2.4. Substrate–consolidant interaction. Substrate–consolidant interactions were determined through Fourier Transform Infrared Spectroscopy (FTIR). With this transmittance technique, the bond between the ceramic substrate and the consolidant can be identified by the identification of new functionalities. The test was performed using an infrared FTIR Prestige 21 spectrometer with a resolution of 4 cm^{-1} and a spectral range of 4000–400 cm^{-1}. Powder samples from the specimens were micronized with ethanol, dried at 40 °C, and combined with KBr powder in a brick-KBr ratio of 1:200 to produce a tablet suitable for measurement.

3. Results and discussion

3.1. Characterization of raw materials

The XRD results from the clay-brick specimens detected quartz and plagioclase (albite in all cases and anorthite in L10-1000), as seen in Fig. 1. Both crystalline forms were also identified in the raw clay prior to calcination. In specimens L10-800 and L20-900, phyllosilicates (illite and muscovite) were identified. On the other hand, L10-1000, the highest calcination temperature specimen, exhibited mineral forms generated by the decomposition of clay minerals under high calcination temperatures, such as mullite ($2SiO_2Al_6O_{13}$). Because this phase was not identified in the raw clay or kaolin XRD results, its presence is attributed to the high-temperature vitrification process. In addition, the appearance of anorthite corroborates the high degree of melting and recrystallization of calcium at this temperature, as it is not found in specimens treated at lower temperatures. In L0-900 and L10-900, phyllosilicates and vitrified phases were not identified. The presence of muscovite in the L20-900 sample is attributed to its higher content of kaolin, which exhibited phyllosilicates in its raw material analysis.

3.2. Consolidation effectiveness assessment

The consolidant retention, expressed as the mass gain compared to the non-consolidated state, was not identical for the different clay bricks, despite all bricks having been immersed in the consolidant for 1 h. The average consolidant retention in the specimens was 5.4%. The specimen microstructure had a significant effect on the level of consolidant retention, as shown in Fig. 2. Samples are organized in the chart by calcination temperature, where at 900 °C 3 different kaolin contents (0–10–20% by wt.) were evaluated.

The consolidant retention decreased as the temperature of calcination increased and it tended to increase as the amount of kaolin increased. Kaolin might facilitate consolidant retention, while calcination temperature modifies brick microstructures unfavorably for consolidation.

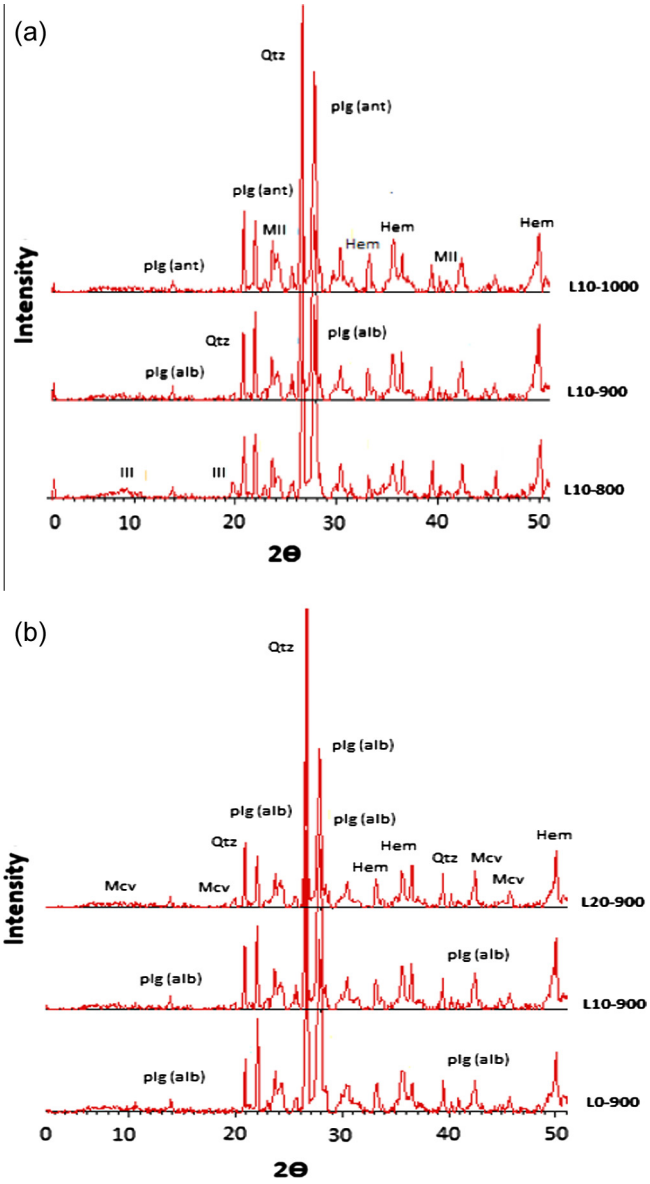

Fig. 1. Diffractograms of the clay-brick specimens according to (a) temperature of calcination and (b) amount of kaolin.

3.2.1. Mechanical properties

Consolidation treatment had a positive effect on surface hardness, as all clay brick specimens tested exhibited decreased surface penetration depth (Fig. 3). The L10-800 and L0-900 specimens achieved the greatest increases in surface hardness, of 59.6% and 51.5%, respectively. The results suggest that there may be a ceiling

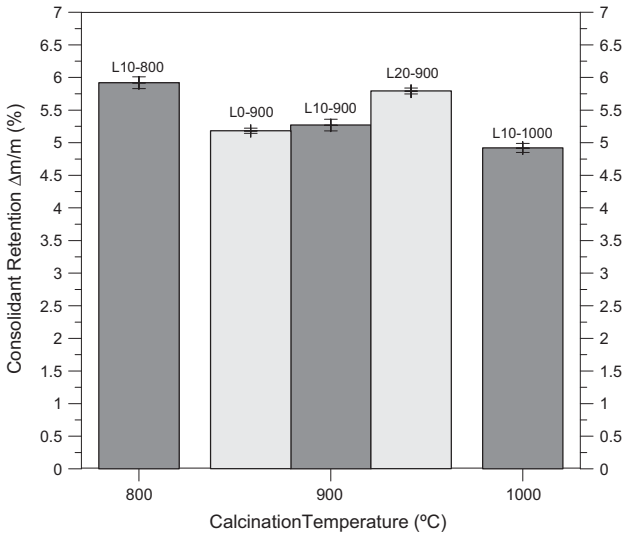

Fig. 2. Consolidant retention of the different clay-brick mixtures tested. Samples are grouped by calcination temperature. At 900 °C, 3 mixtures of different kaolin contents were tested.

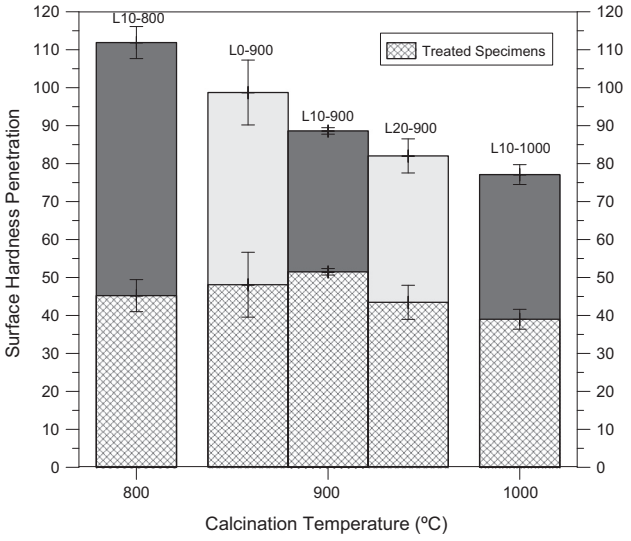

Fig. 3. Surface penetration by a steel ball 6-mm in diameter of non-treated and treated specimens. Treated specimens are plotted over the corresponding non-treated specimen results as hatched bars.

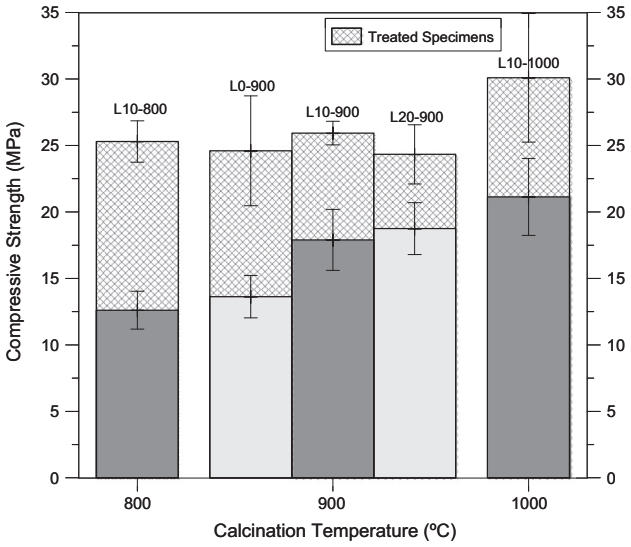

Fig. 4. Compressive strength of non-treated and treated specimens. Treated specimen results are plotted over corresponding non-treated specimen results as hatched bars.

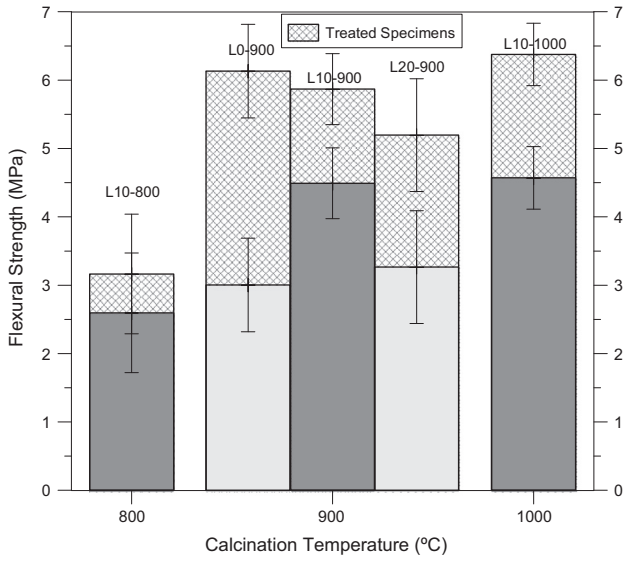

Fig. 5. Flexural strength of non-treated and treated specimens. Treated specimen results are plotted over corresponding non-treated specimen results as hatched bars.

to the hardness of the treated specimens, as all of the specimens reached a hardness value of between 40 and 50 penetration units regardless of their microstructure. This may be attributed to the hardness of the consolidant in those samples.

The results of compressive and flexural strength tests are shown in Figs. 4 and 5, respectively. As can be observed from the measured strengths, prior to consolidation, the compressive and flexural strength increased with increases in calcination temperature and kaolin content.

Statistical hypothesis testing was performed for means comparison between non-treated and treated specimens. The null hypothesis is rejected when the *P*-value for the test is less than 0.05 at the 95% confidence level. Therefore, all of the sample results, except the flexural strength of L10-800, showed significant increases in strength.

With the exception of the flexural strength results of L10-800, the treated specimens had statistically similar compressive and flexural strengths of between 25–30 MPa and 4–6 MPa, respectively. The highest increases in compressive strength were obtained for L10-800 (100.6%) and L0-900 (80.5%). Regarding flexural strength, the highest increases in mechanical performance were obtained for L0-900 (104.1%) and L20-900 (59.1%).

L10-1000 developed the highest average compressive and flexural strengths when treated. However, these samples also exhibited the highest strengths in the non-treated state. Therefore, their high mechanical performance is attributed to a combination of the higher initial strength of the brick matrix, which can be explained by a higher level of vitrification, and the contribution of the consolidant in the treated samples.

Improvements in mechanical performance (Figs. 3–5) are partially explained by consolidant retention (Fig. 2), as the L10-800 specimens, with the highest consolidant retention (5.9%), showed the highest increases in compressive strength. As expected, the ini-

Table 3
Statistical hypothesis testing for means comparison between non-treated and treated specimens.

		t-Value	*P*-Value
L0-900	Compression	−5.539	0.002
	Flexural	−7.222	0.007
L10-800	Compression	−13.437	0.000
	Flexural	−0.971	0.399
L10-900	Compression	−7.305	0.001
	Flexural	−3.724	0.024
L10-1000	Compression	−3.555	0.010
	Flexural	−3.389	0.039
L20-900	Compression	−4.211	0.003
	Flexural	−3.542	0.036

tial mechanical properties of the brick matrix are relevant to the absolute results obtained from the treated samples.

3.2.2. Physical and transport properties

The effectiveness of consolidation treatment can also be evaluated by assessing changes in physical and transport properties (Table 3) such as unit weight, open porosity, electrical resistivity and absorption coefficients when applying the consolidant.

As seen from Table 3, higher calcination temperatures decrease the level of open porosity due to the higher level of vitrification reached in these samples. This finding is consistent with the results observed in Figs. 3–5, where surface hardness, compressive and flexural strength increased with calcination temperature in non-treated samples. Compressive strength is inversely related to porosity [24,25]; thus, bricks with higher initial strength are expected to exhibit lower porosity.

This finding would also explain the lower retention of consolidant in samples calcined at higher temperatures (Fig. 2). Regarding the kaolin effect, there is a slight increase in open porosity as the kaolin level increases. This can also explain the increase in consolidant retention seen in samples with higher amounts of kaolin.

The specific gravity of non-treated specimens is consistent for substrates with high quartz contents (SG_{quartz} = 2.7 g/cm^3), as are present in the clay bricks. In all cases, the unit weights increased. The increases in unit weight, together with the addition of consolidant, corroborated the capacity of the brick matrix to store, and allow the polymerization of, the consolidant. Open porosity decreased with treatment in all cases with specimens L10-800 exhibiting the greatest reduction (7.3%), which is in accordance with their high levels of measured consolidant retention (Fig. 2).

Regarding pore interconnection, non-treated specimens exhibited increased electrical resistivity (equivalent to a decrease in pore interconnectivity) as the temperature of calcination increased (increased vitrification and reduced open porosity) or the content of kaolin decreased (a slight reduction in open porosity) as shown in Table 4. This trend was also present in the treated specimens. In general, all clay brick specimens exhibited increased electrical resistivity when treated with the consolidant. L10-1000 exhibited the greatest increases in electrical resistivity (45%) and L0-900 exhibited the lowest (7%). However, the results for L0-900 are considered outliers.

Table 4
Transport properties of non-treated and treated specimens.

Clay brick type	Treatment	Open porosity (%)	Electrical resistivity (Ω m)	Initial rate of water absorption (mm/s$^{1/2}$)
L0-900	Non-treated	31.4	71	0.330
	Treated	24.5	76	0.026
L10-800	Non-treated	31.4	47	0.220
	Treated	24.1	62	0.060
L10-900	Non-treated	31.1	54	0.320
	Treated	25.1	67	0.029
L10-1000	Non-treated	30.6	64	0.490
	Treated	24.2	93	0.052
L20-900	Non-treated	31.5	44	0.310
	Treated	24.6	62	0.090

All non-treated specimens exhibited similar capillary absorption behavior (dashed-line curves in Fig. 6). This behavior included a sharp increase during the first 2 h, representing the high interconnectivity of the porosity of the bricks (slope represented by the initial rate of water absorption, presented in Table 3). This was followed by a second slow-absorption stage, with final absorption values of approximately 14 to 15 mm, which represent the total accessible porosity. Fig. 6a shows the results for non-treated (dashed line) and treated (continuous line) samples calcined at different temperatures with 10% kaolin content, while Fig. 6b shows the results for samples calcined at 900 °C with different kaolin compositions.

Treatment with consolidant produced a significant reduction in the capillary absorption of all clay brick specimens (solid-line curves in Figs. 6a and b), leading to final absorption coefficients of approximately 10 mm for all samples, compared to the 14–15 mm of non-treated samples. This is consistent with the reduction in open porosity and pore connectivity observed in treated samples compared to non-treated bricks.

Fig. 6a shows that, as calcination temperature increases, the water uptake of treated samples accelerates. However, samples L10-1000 reached an equilibrium absorption value that was slightly lower than samples calcined at 800 or 900 °C. In addition, samples L10-1000 samples exhibited the highest strength and hardness values measured in both non-treated and treated states (Figs. 3–5) and consistently exhibited the lowest open porosity levels (Table 3). Capillary absorption is dominated by the radius and volume of the unsaturated pores [22]. This suggests that vitrification interacts with the initial clay brick structure to reduce the total pore volume. Therefore, open porosity decreases and mechanical properties are enhanced. Similarly, consolidant retention is lower as the total pore volume is reduced.

Sample pre-conditioning is critical to ensure that the initial humidity of the samples prior to testing is at equilibrium. As the pre-conditioning procedure followed corresponds to a method designed for concrete samples, which exhibit different pore size distributions than clay bricks, some effects of this "moisture history" [22] could also explain the behavior of samples L10-1000, as smaller pores require higher-lower RH exposures to saturate or empty, respectively.

Fig. 6a shows that, as the kaolin level increases, water uptake is also accelerated. This finding is corroborated by the retention and open porosity results, as higher levels of open porosity were observed as kaolin content increased (Table 3), leading to greater retention (Fig. 2).

Pore size distribution is also significantly affected by consolidation treatment (Fig. 7).

The results show that, in pores ranging in size between 1 and 0.1 μm, the lowest reduction, 8%, was obtained by the L10-800 specimens, while the largest, 23%, was obtained by the L10-1000 specimens. Likewise, in pores ranging in size between 0.1 and 0.01 μm, the lowest reduction, 10%, was obtained by specimens L10-1000, specimens while the largest, 28%, was obtained by specimens L10-800.

In the gel pore range (<0.01 μm), all specimens except L10-1000 exhibited an increase after treatment. This could be explained by an increase in the residual microporosity due to the porosity of the consolidant and microcracking due to capillary forces and gelification stresses during curing [26].

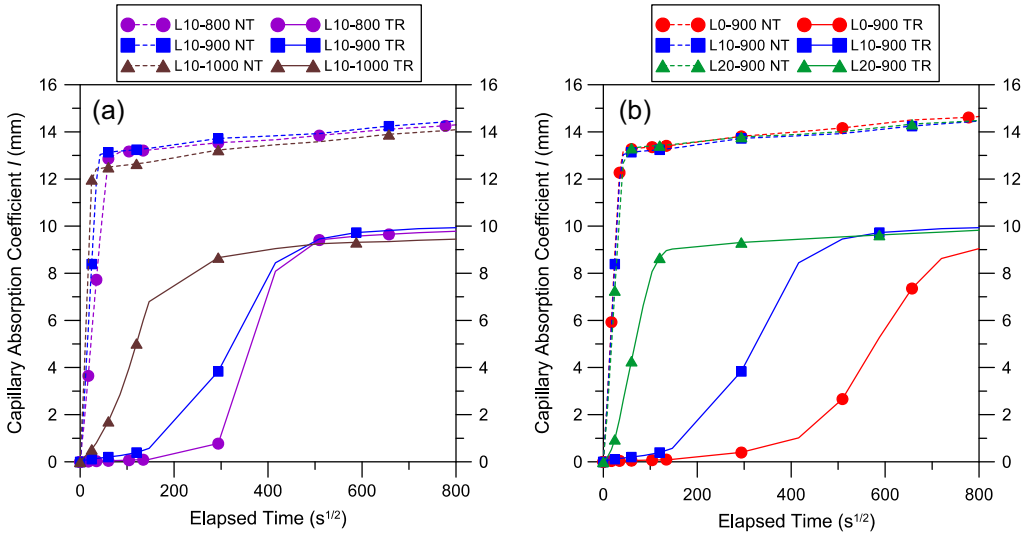

Fig. 6. Water capillary absorption. (a) Samples with 10% kaolin calcined at 800–900–1000 °C (b) Samples calcined at 900 °C with 0–10–20% kaolin.

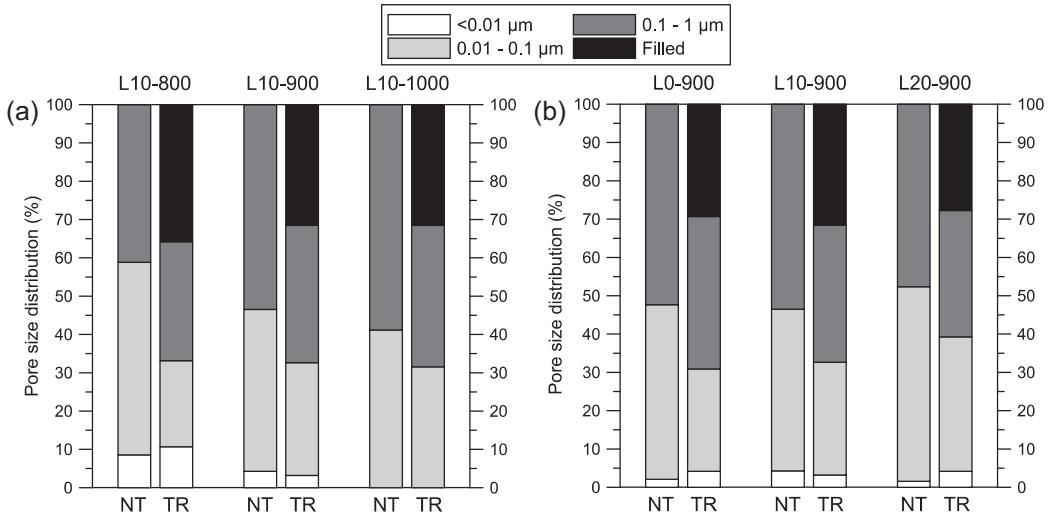

Fig. 7. Pore size distribution of the non-treated and treated specimens according to (a) temperature of calcination and (b) amount of kaolin (NT: Non-treated and TR: Treated).

Larger improvements in mechanical and transport properties were achieved in specimens in which greater reductions in pore size were observed (L10-800 and L0-900). This is in agreement with the results and conclusions of Ferreira and Delgado [27], who proposed that the deposition of SiO_2 formed during consolidant application precipitates initially in the capillary pores, causing a strengthening of the grains and the contacts among them. On the other hand, the effects on specimens in which smaller pore size reductions were observed (L10-1000 and L20-900) were lower and are related to the pore filling effect.

In general, the reductions achieved in this pore range benefit the durability of the bricks because materials with abundant pores within this range are susceptible to problems caused by the crystallization of salts, freeze–thaw cycles and gas attacks [12,28].

3.2.3. Aesthetic properties

Color change can be important in some historical buildings and can occur after treatment with consolidant. Non-treated (NT) specimens were used as references for the calculation of chromatic variables. A reduction in the luminosity factor L^*, was observed in all treated specimens ($L_2^* < L_1^*$), which quantifies a darkening

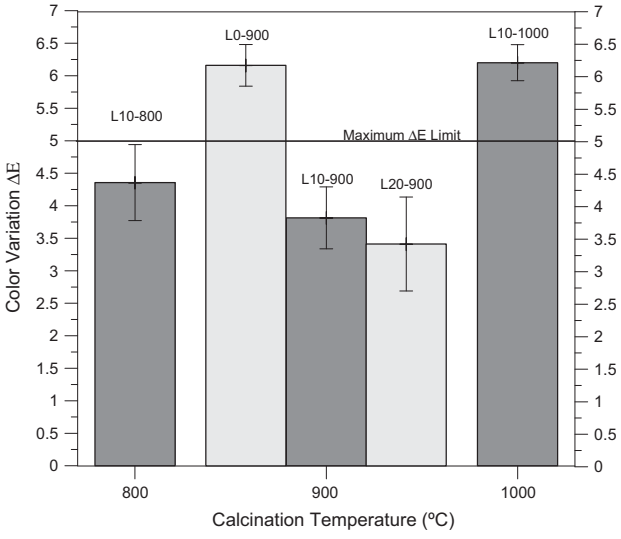

Fig. 8. Color variation between treated and non-treated samples after consolidation. (NT: Non- treated, TR: Treated).

effect. Small reductions in chromatic coordinates a^* and b^* were detected in relation to their initial values. The literature proposes [29,30] an acceptable limit of $\Delta E < 5$ in the color change of treated specimens (TR), due to aesthetical considerations (Fig. 8). Following this recommendation, specimens with higher hematite content (higher a^* values) exceeded the recommended limit. Thus, testing in a small hidden area of the structure is recommended to evaluate color change effects prior to the application of the consolidant.

3.2.4. Substrate–consolidant interaction

The effect of consolidation can be represented, through an FTIR test, by variations in the functional bands in specific groups between non-treated and treated specimens. The main groups of interest for this study are shown in the functional bands of Fig. 9 [10,29,31,32].

A comparison of non-treated and treated specimens revealed an increase or the appearance of the OH band in all cases. Likewise, the increase in the Si–O–Si bands located at 1040, 780 and 462 cm^{-1} frequencies can be explained by the creation of new Si–O–Si bonds after polymerization. The shift of the bands located at 1020–1040 cm^{-1} toward 1100 cm^{-1} can also be explained by the formation of new Si–O–Si bonds within the hydrolyzed silicate [32]. The reduction in Si–O–Al bands, located at the wavelengths 640 and 586 cm^{-1}, also implies interactions between the aluminosilicate groups and the Si–O–Si groups of the consolidant.

Increases in mechanical properties, especially flexural strength, can be explained by the presence of bonds between the substrate and the consolidant. Specifically, for specimens L10-800, the interaction between consolidant and substrate is expected to be greater due to the presence of a larger number of available OH groups, which form after the hydrolization of the ethyl silicate consolidant alkoxy groups, and phyllosilicates, which form due to the low calcination temperature. The increased presence of Si–OH bonds in samples L10-800 may be attributed to increased consolidant retention compared to samples L10-1000 (Fig. 2).

The appearance of Si–O–C bonds in both treated and non-treated samples suggests that, at the time of testing, the polymerization process had not concluded, and thus more curing time was required to achieve the maximum performance associated with consolidant retention in the brick matrix. This conclusion is also

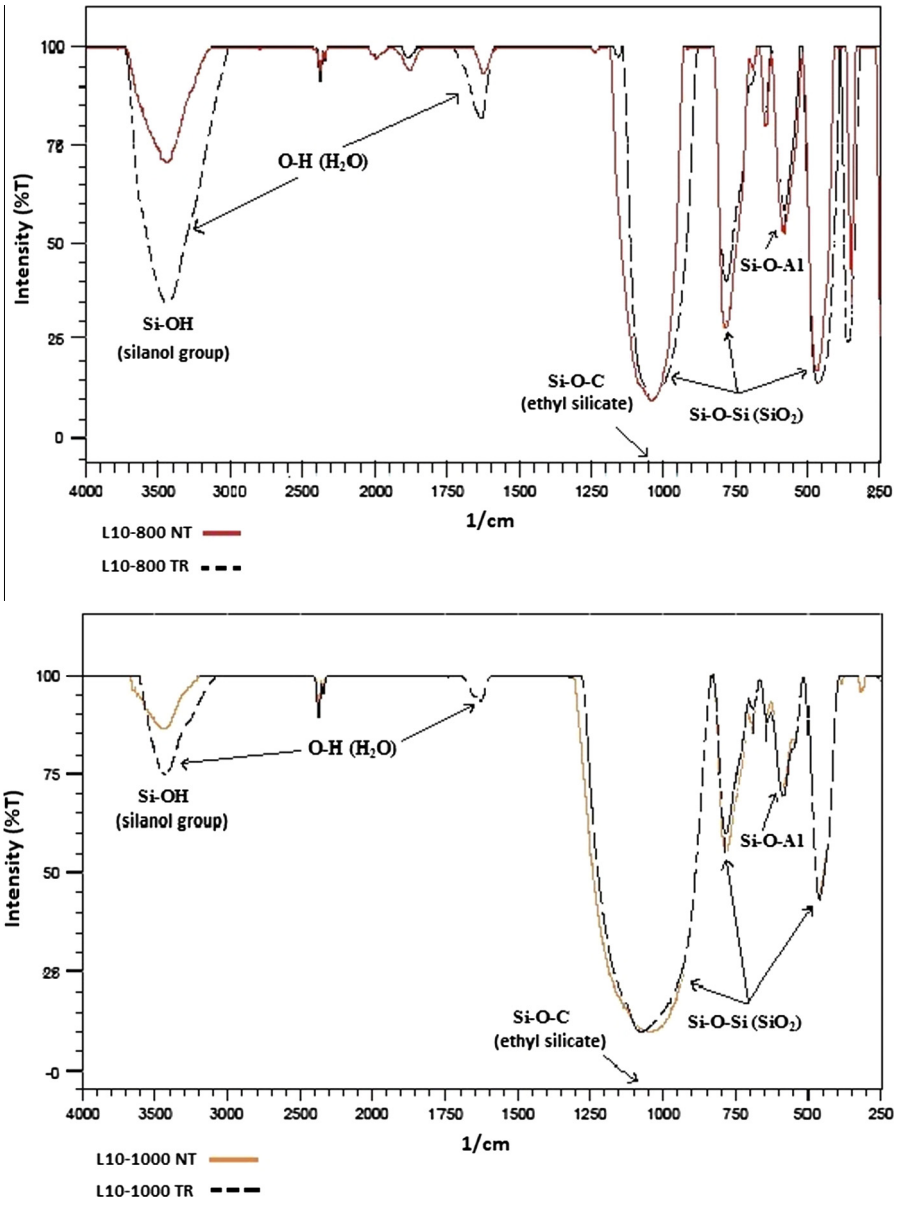

Fig. 9. Location of primary bands of interest and detection of the variations obtained in samples L10-800 and L10-1000. (NT: Non- treated, TR: Treated).

supported by the presence of Si–OH groups in the treated samples. In both cases, evidence of variation in the intensity of Si–O–Si bonds between treated and non-treated samples verifies some degree of polymerization of the consolidant.

Thus, the improvements in mechanical and transport properties achieved in the clay brick specimens are due to two effects of ethyl silicate in the substrate: (a) the deposition of the consolidant in the pores (porosity filling/reduction effect) and (b) the substrate–consolidant chemical interaction.

4. Conclusions

Fired-clay bricks are the primary construction material used in heritage structures. To improve their mechanical and transport properties, consolidation with TEOS has gained popularity due to its effectiveness and architectural neutrality with the existent surface finish. This study assessed the effects of TEOS on the substrate quality of bricks manufactured with different clay-kaolin ratios and at different firing temperatures and on consolidation effectiveness measured as mechanical and transport properties. Samples were treated by immersion in TEOS for 1 h, and were allowed to reach equilibrium RH with the ambient atmosphere prior to testing.

All treated specimens exhibited improved mechanical and transport properties, suggesting that consolidation with ethyl silicate is effective. However, the improvements obtained strongly depend on the initial properties of the bricks, given by the initial porosity of the samples, which strongly influenced the retention of consolidant.

Treated specimens that achieved higher consolidant retention also exhibited greater improvements in mechanical and transport properties. In addition, calcination temperature was found to reduce open porosity, thus improving the initial mechanical properties of the non-treated samples and reducing consolidant retention. Thus, consolidation effectiveness (as measured by the variation between treated and non-treated samples) is directly dependent on brick porosity, while mechanical and transport properties are also strongly related to the properties of non-treated bricks.

Substrate–consolidant bonds were detected using FTIR, which can explain observed the increase in flexural strength. Microstructures with greater number of accessible O–H groups (for low calcination temperature or higher humidity) developed an increased amount of polymerized Si–O–Si matrix due to higher levels of hydrolization.

Improvements in mechanical and transport properties achieved in treated samples, as well as the detection of a substrate–consolidant interaction by FTIR, demonstrate an improvement in the durability of the substrate bricks. These effects demonstrate that the consolidation effectiveness is closely related to the microstructure of the specimen (mainly its open porosity) and substrate–consolidant interaction (mineralogy).

Consolidation with ethyl silicate resulted in alterations to chromatic properties that were not significant in most treated specimens. For bricks with high hematite content, special considerations should be taken and sample consolidation and color variation testing must be conducted prior to the selection of the most suitable procedure and consolidant product to be used.

The immersion procedure selected for brick consolidation differs significantly from real practice. This procedure was selected to ensure the same availability of consolidant in all the tested bricks, to assess the effect of brick microstructure on consolidation and retention. Thus, the results presented herein may be considered referential indicators of the effect of consolidation on mechanical and transport properties with different brick porosities.

Acknowledgements

We thank Wacker Chemie for providing the consolidant and Industrias Princesa Ltda. for supplying the raw materials used to produce the specimens tested. We also thank Gloria Arancibia of the Department of Structural and Geotechnical Engineering and Pablo Pastén of the Department of Hydraulic and Environmental Engineering of the Pontificia Universidad Católica de Chile, and Diego Morata and Mercedes Vázquez, for characterizing the raw materials and manufactured specimens. Finally, we are thankful for the support provided by project CONICYT–FONDEF ID14I10187 and project CONICYT–FONDAP 15110020 (Center of Sustainable Urban Development/CEDEUS).

References

[1] P.S. Nayak, B.K. Singh, Instrumental characterization of clay by XRF, XRD and FTIR, Bull. Mater. Sci. 30 (2007) 235–238, http://dx.doi.org/10.1007/s12034-007-0042-5.
[2] G. Cultrone, F. Madkour, Evaluation of the effectiveness of treatment products in improving the quality of ceramics used in new and historical buildings, J. Cult. Herit. 14 (2013) 304–310, http://dx.doi.org/10.1016/j.culher.2012.08.001.
[3] G. Görhan, O. Şimşek, Porous clay bricks manufactured with rice husks, Constr. Build. Mater. 40 (2013) 390–396, http://dx.doi.org/10.1016/j.conbuildmat.2012.09.110.
[4] C. Cennamo, Fiore.M. Di, Structural, seismic and geotechnical analysis of the Sant' Agostino church in L'aquila (Italy), Rev. Ing. Constr. RIC 28 (2013) 7–20, http://dx.doi.org/10.4067/SO718-50732013000100001.
[5] Ilustre Municipalidad de Santiago, Catalogo de Inmuebles de Conservación Histórica, 2014.
[6] S. Meseguer, F. Pardo, M.M. Jordan, T. Sanfeliu, I. González, Ceramic behaviour of five Chilean clays which can be used in the manufacture of ceramic tile bodies, Appl. Clay Sci. 47 (2010) 372–377, http://dx.doi.org/10.1016/j.clay.2009.11.056.
[7] K. Elert, G. Cultrone, C. Rodriguez Navarro, E. Sebastián Pardo, Durability of bricks used in the conservation of historic buildings – Influence of composition and microstructure, J. Cult. Herit. 4 (2003) 91–99, http://dx.doi.org/10.1016/S1296-2074(03)00020-7.
[8] I.N. Paes, E. Bauer, H. Carasek, E. Pavón, Influence of water transportation inside a mortar/block system on bonding resistance behavior, Rev. Ing. Constr. RIC 29 (2014) 175–186, http://dx.doi.org/10.4067/S0718-50732014000200004.
[9] E. Franzoni, B. Pigino, A. Leemann, P. Lura, Use of TEOS for fired-clay bricks consolidation, Mater. Struct. 47 (2014) 1175–1184, http://dx.doi.org/10.1617/s11527-013-0120-7.
[10] F. Sandrolini, E. Franzoni, B. Pigino, Ethyl silicate for surface treatment of concrete – Part I: Pozzolanic effect of ethyl silicate, Cem. Concr. Compos. 34 (2012) 306–312, http://dx.doi.org/10.1016/j.cemconcomp.2011.12.003.
[11] Industrias Princesa, Personal interviews and technical visits at the clay-brick Factory of Industrias Princesa Ltda, 2013.
[12] G. Cultrone, E. Sebastián, M.O. Huertas, Durability of masonry systems: a laboratory study, Constr. Build. Mater. 21 (2007) 40–51, http://dx.doi.org/10.1016/j.conbuildmat.2005.07.008.
[13] P. López-Arce, Ladrillos de edificios históricos de Toledo: Caracterización, origen de las materias primas y aplicaciones para su conservación y restauración, Universidad Complutense de Madrid, 2004.
[14] G. Cultrone, E. Sebastián, K. Elert, M.J. de la Torre, O. Cazalla, C. Rodriguez-Navarro, Influence of mineralogy and firing temperature on the porosity of bricks, J. Eur. Ceram. Soc. 24 (2004) 547–564, http://dx.doi.org/10.1016/S0955-2219(03)00249-8.
[15] P. Blanc, O. Legendre, E.C. Gaucher, Estimate of clay minerals amounts from XRD pattern modeling: the Arquant model, Phys. Chem. Earth 32 (2007) 135–144, http://dx.doi.org/10.1016/j.pce.2006.03.004.
[16] UNE-EN 1926:2007, Métodos de ensayo para la piedra natural. Determinación de la resistencia a la compresión uniaxial, n.d.
[17] UNE-EN 12372:2007, Métodos de ensayo para piedra natural. Determinación de la resistencia a la flexión bajo carga concentrada, n.d.
[18] UNE-EN 1936:2007, Métodos de ensayo para la piedra natural. Determinación de la densidad real y aparente y de la porosidad abierta y total, n.d.
[19] UNE-EN-1925:1999 Métodos de ensayo para la piedra natural. Determinación del coeficiente de absorción de agua por capilaridad, n.d.
[20] ASTM C1585-13, Standard Test Method for Measurement of Rate of Absorption of Water by Hydraulic-Cement Concretes, n.d.
[21] J.F. Straube, E.F.P. Burnett, Building Science for Building Enclosures, Building Science Press, 2005.
[22] J. Castro, R. Spragg, J. Weiss, Crack-healing investigation in bituminous materials, J. Mater. Civ. Eng. 25 (2013) 864–870, http://dx.doi.org/10.1061/(ASCE)MT.1943-5533.
[23] ASTM E104-02, Standard, Practice for Maintaining Constant Relative Humidity by Means of Aqueous Solutions, n.d.

[24] P. Mehta, P. Monteiro, Concrete: Microstructure, Properties and Materials, third ed., McGraw-Hill Professional, New York, 2005.
[25] A. Neville, Properties of Concrete, fourth ed., Pearson Education Limited, Essex, 1995.
[26] R. Zárraga, J. Cervantes, C. Salazar-Hernandez, G. Wheeler, Effect of the addition of hydroxyl-terminated polydimethylsiloxane to TEOS-based stone protective materials, J. Cult. Herit. 11 (2010) 138–144, http://dx.doi.org/10.1007/s10971-012-2926-0.
[27] A.P. Ferreira Pinto, J. Rodrigues Delgado, Stone consolidation: the role of treatment procedures, J. Cult. Herit. 9 (2008) 38–53, http://dx.doi.org/10.1016/j.culher.2007.06.004.
[28] K. Elert, G. Cultrone, C. Rodriguez Navarro, E. Sebastián Pardo, Durability of bricks used in the conservation of historic buildings – influence of composition and microstructure, J. Cult. Herit. 4 (2003) 91–99.
[29] P. Maravelaki-Kalaitzaki, N. Kallithrakas-Kontos, Z. Agioutantis, S. Maurigiannakis, D. Korakaki, A comparative study of porous limestones treated with silicon-based strengthening agents, Prog. Org. Coat. 62 (2008) 49–60, http://dx.doi.org/10.1016/j.porgcoat.2007.09.020.
[30] J.D. Rodrigues, A. Grossi, Indicators and ratings for the compatibility assessment of conservation actions, J. Cult. Herit. 8 (2007) 32–43, http://dx.doi.org/10.1016/j.culher.2006.04.00.
[31] J.A. Calabria, W.L. Vasconcelos, A.R. Boccaccini, Microstructure and chemical degradation of adobe and clay bricks, Ceram. Int. 35 (2009) 665–671, http://dx.doi.org/10.1016/j.ceramint.2008.01.02.
[32] C. Kapridaki, P. Maravelaki-Kalaitzaki, TiO_2–SiO_2-PDMS nano-composite hydrophobic coating with self-cleaning properties for marble protection, Prog. Org. Coat. 76 (2013) 400–410, http://dx.doi.org/10.1016/j.porgcoat.2012.10.006.